

See discussions, stats, and author profiles for this publication at: <https://www.researchgate.net/publication/231462502>

The equilibrium constant and rate constant for allyl radical recombination in the gas phase

ARTICLE *in* JOURNAL OF THE AMERICAN CHEMICAL SOCIETY · FEBRUARY 1979

Impact Factor: 12.11 · DOI: 10.1021/ja00499a029

CITATIONS

69

READS

39

3 AUTHORS, INCLUDING:



Michel J Rossi

Paul Scherrer Institut

259 PUBLICATIONS 6,494 CITATIONS

SEE PROFILE

The algorithm and program for symmetry group finding were provided by Dr. Harold Brown. Programming assistance was provided by Mr. Frederick Fisher. Editorial assistance was provided by Helen K. Tognetti. Manuscript preparation assistance was provided by Janet Kay Friendshuh. Financial support was provided by the National Institutes of Health Grant 2R24 R 00612-08.

Appendix

Constitution and Constitutional Isomer. The constitution of a chemical structure is defined as the set of atoms and the set of bonds connecting them. For any pair of atoms there is an integral number of bonds from 0 to 3 connecting them. Constitutional isomers have the same set of atoms but differ in the set of bonds.

Order of a Group. The order is the number of elements in the group.

Orbits of a Permutation. The orbits are the sets of atoms made equivalent by the permutation. The permutation (123) (4) has two orbits, one of length 3 and one of length 1.

Even or Odd Permutations. For the symmetry group of the tetrahedron, even permutations are of the type (1) (2) (3) (4),

(12) (34), (123) (4), and odd permutations are of the type (12) (3) (4) and (1234). (See ref 3 for further details.)

References and Notes

- (1) Applications of Artificial Intelligence for Chemical Inference. 29. For part 28 see J. G. Nourse, *J. Am. Chem. Soc.*, preceding paper in this issue.
- (2) (a) L. M. Mastiner, N. S. Sridharan, J. Lederberg, and D. H. Smith, *J. Am. Chem. Soc.*, **96**, 7702 (1974); (b) L. M. Mastiner, N. S. Sridharan, R. E. Carhart, and D. H. Smith, *ibid.*, **96**, 7714 (1974); (c) R. E. Carhart, D. H. Smith, H. Brown, and C. Djerassi, *ibid.*, **97**, 5755 (1975); (d) R. C. Read in "Chemical Applications of Graph Theory", A. T. Balaban, Ed., Academic Press, New York, 1976, Chapter 4.
- (3) J. G. Nourse, *J. Am. Chem. Soc.*, preceding paper in this issue.
- (4) H. Brown, *SIAM J. Appl. Math.*, **32**, 534 (1977).
- (5) F. A. Cotton, "Chemical Applications of Group Theory", 2nd ed., Wiley-Interscience, New York, 1971.
- (6) W. T. Wipke and T. M. Dyott, *J. Am. Chem. Soc.*, **96**, 4834 (1974).
- (7) Technically, this smaller group is a homomorphic image of the larger one.
- (8) R. S. Cahn, C. Ingold, and V. Prelog, *Angew. Chem., Int. Ed. Engl.*, **5**, 385 (1966).
- (9) C. H. Park and H. E. Simmons, *J. Am. Chem. Soc.*, **94**, 7184 (1972).
- (10) G. Schill, "Catenanes, Rotaxanes, and Knots", Academic Press, New York, 1971.
- (11) R. A. Davidson, Ph.D. Thesis, The Pennsylvania State University, 1976.
- (12) J. G. Nourse, to appear.
- (13) L. T. Scott and M. Jones Jr., *Chem. Rev.*, **72**, 181 (1972).
- (14) H. W. Whitlock and M. W. Siefken, *J. Am. Chem. Soc.*, **90**, 4929 (1968).
- (15) T. H. Varkony, R. E. Carhart, and D. H. Smith in "Computer-Assisted Organic Synthesis", W. T. Wipke and W. J. Howe, Eds., ACS Symposium Series No. 61, 1977, p 188.
- (16) V. Prelog and H. Gerlach, *Helv. Chim. Acta*, **47**, 2288 (1964).

The Equilibrium Constant and Rate Constant for Allyl Radical Recombination in the Gas Phase

M. Rossi,[†] K. D. King,[‡] and D. M. Golden*

Contribution from the Thermochemistry and Chemical Kinetics Group, SRI International, Menlo Park, California 94025. Received May 4, 1978

Abstract: The equilibrium and recombination $2 \text{ allyl} \rightleftharpoons 1,5\text{-hexadiene}$ at $\langle T \rangle = 950 \text{ K}$ and the recombination reaction at $T = 625 \text{ K}$ have been studied in a VLPP (very low-pressure pyrolysis) apparatus. The van't Hoff plot yields $\ln K_{\text{r,d}}/M^{-1} = (-34.56 + 10.60)/R + (56.100/RT)$, which gives $\Delta H^\circ_{\text{r}}(\text{allyl}) = 39.1 \pm 1.5 \text{ kcal/mol}$, a bond dissociation energy $\text{BDE}(\text{C}_3\text{H}_5\text{-H}) = 86.3 \pm 1.5 \text{ kcal/mol}$, and an allyl resonance energy $\text{ARE} = 11.7 \pm 2.0 \text{ kcal/mol}$. The recombination rate constant k_{r} at $\langle T \rangle = 900 \text{ K}$ is found to be $(1.90 \pm 0.80) \times 10^9 \text{ M}^{-1} \text{ s}^{-1}$, and at $T = 625 \text{ K}$, k_{r} is $(6.50 \pm 1.0) \times 10^9 \text{ M}^{-1} \text{ s}^{-1}$. RRKM calculations indicate a degree of fall-off $k_{\text{r}}/k_{\text{r}}^\infty = 0.37$ at 625 K and 0.045 at 900 K.

I. Introduction

Allyl radical is the prototype of a resonance-stabilized radical whose thermochemistry and reactivity in the gas phase have been the subject of numerous investigations.¹⁻³ There has been considerable controversy^{1a} about the correct value of the heat of formation and the allyl resonance energy (ARE).⁴ Quoted values for ARE range from 10 to 25 kcal/mol, but recent experimental values for ARE now seem to fall around $11 \pm 2 \text{ kcal/mol}$. The correct value for ARE is certainly fundamental for a thorough understanding of chemical bonding and ground-state properties of conjugated radicals. Theoretical calculations on open-shell species, such as allyl radical, are hampered somewhat by intrinsic difficulties,⁵ but, despite this problem, the generalized valence-bond (GVB) concept appears to be quite successful.⁶

Furthermore, the need for the accurate determination of radical-radical recombination rate constants has been clearly pointed out.⁷ Absolute rate constants for many dispropor-

tionation reactions and radical-molecule reactions are critically dependent on the rates for combination of the radicals, since many rate constants have been measured relative to the radical combination rate constants. Thermochemical parameters of free radicals can also be obtained from the Arrhenius parameters of free-radical combination in cases where the reverse reaction (dissociation) has been studied. Radical recombination rate studies in the case of resonance-stabilized radicals are sparse and the rates for allyl and 2-methylallyl recombination have only been measured at ambient temperature by flash photolysis.^{8,9} It seemed appropriate to extend the rate measurements in order to get a reliable set of Arrhenius parameters for allyl recombination at higher temperatures where this reaction is the prototype for important chain terminations.

In this paper, we report (a) the equilibrium and kinetics of allyl radical recombination at $844 \text{ K} \leq T \leq 1061 \text{ K}$, and (b) the recombination kinetics of allyl radical at $T = 625 \text{ K}$. The method used is very low-pressure pyrolysis (VLPP) employing a newly designed molecular beam sampling apparatus, thereby eliminating complicated secondary reactions of radicals on the walls of the mass spectrometry chamber.¹⁰

[†] Postdoctoral Research Associate.

[‡] On leave from Department of Chemical Engineering, University of Adelaide, Adelaide, South Australia 5001.

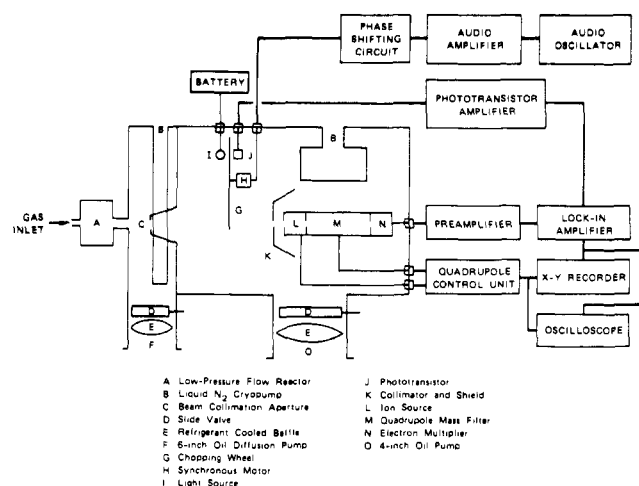


Figure 1. Block diagram for experimental setup of VLPP (very low-pressure pyrolysis) experiment.

II. Experimental Section

Figure 1 depicts the general experimental design of the molecular beam-sampling VLPP apparatus. A valve-capillary tube arrangement delivers a controlled, steady flow of reactant gas to the reactor (typically, 10^{13} to 5×10^{16} molecules/s). In cases where the reactant gas had an unsuitably low vapor pressure at room temperature, the whole gas inlet system was placed in a hot box. The flow then enters the low-pressure reactor and subsequently effuses from the reactor exit aperture. The product gas flux is collimated (<1 cm in diameter) on passing through a differential pumping chamber, modulated with a rotating chopper wheel, and finally ionized and detected by a quadrupole mass spectrometer (Finnigan 400). A lock-in amplifier (Princeton Applied Research Model 128A) separates the modulated signal from the unmodulated background signal. Figure 2 displays the two-aperture reactor design. Reactor parameters are given by (B = large aperture, S = small aperture) $V = 0.134$ L, $\omega = 4982(T/M)^{1/2} \text{ s}^{-1}$, $k_e^M(B) = 2.5571(T/M)^{1/2} \text{ s}^{-1}$, $k_e^M(S) = 0.2088(T/M)^{1/2} \text{ s}^{-1}$. The all-quartz reactor (i.e., Knudsen cell) encased in a nickel block was heated with an electrical clam-shell heater, and the temperature was measured by a chromel-alumel thermocouple. The experiments were carried out by monitoring mass spectrometric intensities as a function of the temperature, the flow rate of the gas into the reactor (F_M^i , molecules s^{-1}), and the residence time of the molecules within the reactor (small or large aperture).¹¹ Diallyl oxalate ($\text{C}_3\text{H}_5\text{OCOCOCOC}_3\text{H}_5$) was purchased from Pfaltz and Bauer, Inc., and was purified simply by pumping off all lower boiling fractions (mainly $\text{CH}_2=\text{CHCH}_2\text{CHO}$) at 10^{-3} Torr. GC-MS analysis revealed no further impurities present. 3,3'-Azo-1-propene ($\text{C}_3\text{H}_5\text{N}_2\text{C}_3\text{H}_5$) was prepared according to literature procedures.¹² (The samples contained H_2O and diethyl ether which did not interfere with our measurements. The concentration of 3,3'-azo-1-propene was measured by monitoring m/e 28 in the absence of the molecular ion of $\text{C}_3\text{H}_5\text{N}_2\text{C}_3\text{H}_5$ at m/e 110.)

The reactions were all studied in a reaction vessel which was "cleaned" after every set of two to three experiments (flow rate studies) by passing air through the vessel at temperatures around 1100 K. This procedure served to remove the soot which was formed at high temperatures (1100 K) and could be seen on the walls of the reaction vessel. Such a procedure was necessary because the carbon coating greatly enhanced the interference by heterogeneous reactions.

III. Results and Discussion

A. Equilibrium and Kinetics ($844 \text{ K} \leq T \leq 1061 \text{ K}$). In the range $844 \text{ K} \leq T \leq 1061 \text{ K}$, the following reaction system was studied using diallyl oxalate, $\text{C}_8\text{H}_{10}\text{O}_4$ (DAO), as a convenient source of allyl radicals:¹³

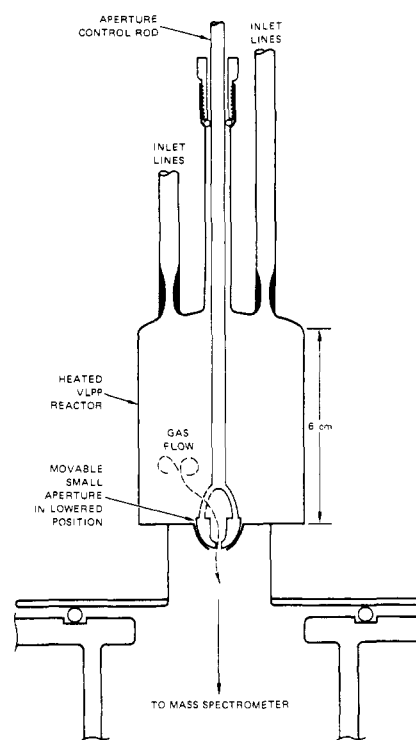
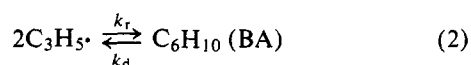
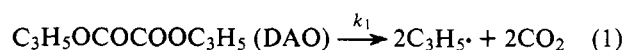
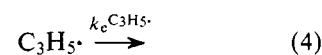
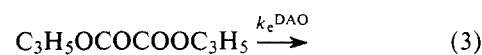
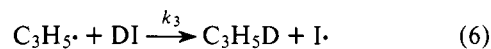


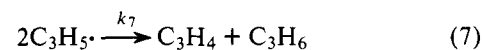
Figure 2. Very low-pressure pyrolysis reactor (133.5 cm^3).



CO_2 served as an internal standard or monitor for allyl radical, because for every allyl radical a molecule of CO_2 was formed. This was verified experimentally by "titrating" $\text{C}_3\text{H}_5\cdot$ with DI:



For $[\text{DI}]_{ss} \geq 5 \times 10^{-8} \text{ M}$, it was verified that $[\text{C}_3\text{H}_5\text{D}]_{ss} = [\text{CO}_2]_{ss}$ through independent calibrations with propylene and CO_2 . Furthermore, this is an experimental demonstration that the formation of 1,5-hexadiene proceeds through recombination of intermediate allyl radicals and not through unimolecular elimination from DAO. It was found that the disproportionation reaction (7) is not important under our experimental conditions:



a conclusion further confirmed by the absence of sizable amounts of allene⁷ and by the results of the Brauman plot (vide infra).

The steady-state kinetic expression for the reaction system (1) to (5) in a low-pressure stirred flow reactor is (see Appendix for details of the derivation)

$$\frac{k_r}{k_d + k_e \text{ BA}} = k_e \text{ BA} \frac{2R_{\text{BA}}^0}{(R_{\text{CO}_2}^0 - 2R_{\text{BA}}^0)^2} \equiv k_e \text{ BA} y \quad (8)$$

where $k_e \text{ BA}$ is the escape rate constant (in s^{-1}) for 1,5-hexadiene (BA), R_{BA}^0 is the specific flow rate (in $\text{mol s}^{-1} \text{ L}^{-1}$) of BA out of the reactor (as monitored by m/e 67 or 54),¹⁴ and $R_{\text{CO}_2}^0$ is the corresponding flow of CO_2 (as monitored by m/e 44).¹⁴ Two experiments, each with different $k_e \text{ BA}$ (or residence

Table I. Equilibrium and Rate Constant Measurements in the Gas Phase Using VLPP

$2\text{C}_3\text{H}_5 \cdot \xrightleftharpoons[k_d]{k_r} \text{C}_6\text{H}_{10}$			
T/K	k_d/s^{-1}	$k_r/\text{M}^{-1} \text{s}^{-1}$	$K_{r,d}/\text{M}^{-1}$
844		2.17×10^9	
845		2.05×10^9	
858	2.72	1.04×10^9	3.83×10^8
888	3.33	1.06×10^9	3.19×10^8
895	18.40	2.40×10^9	1.31×10^8
900	18.55	3.24×10^9	1.75×10^8
922	13.75	1.53×10^9	1.11×10^8
927			7.30×10^7
946			6.81×10^7
975			2.63×10^7
988			1.94×10^7
988			1.42×10^7
990			1.63×10^7
991			1.60×10^7
1057			1.53×10^6
1061			9.51×10^5

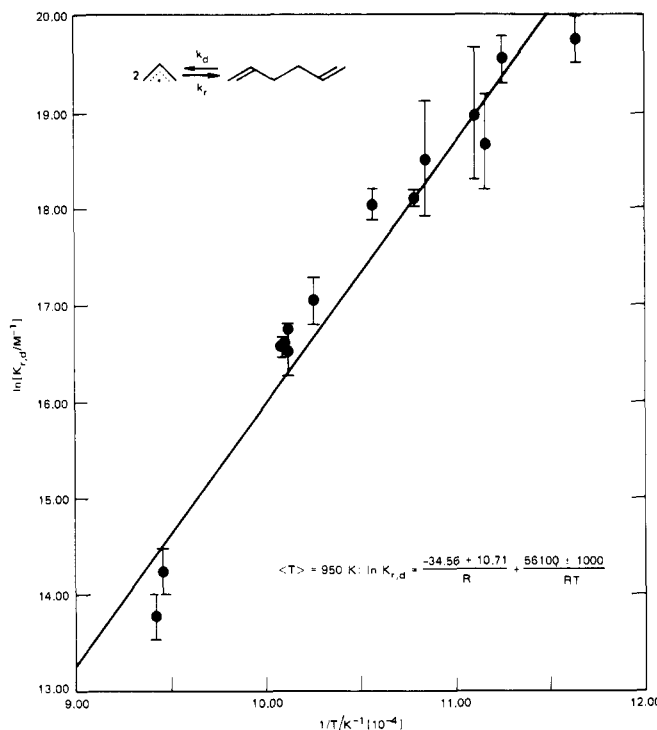
time), were performed at a given temperature, varying F_{DAO} typically from 10^{15} to 4×10^{16} molecules s^{-1} , so that k_r and k_d could be determined separately, but this was possible only over a limited temperature range. Table I displays the results obtained over the temperature range (844–1061 K) and Figure 3 shows the corresponding “third law” van’t Hoff plot for $K_{r,d}$ by assuming an entropy difference ΔS° for equilibrium (2) of -34.80 eu at $\langle T \rangle = 950$ K.^{17,18} The results of the least-squares analysis can be summarized as follows:

$$\ln K_{r,d}/\text{M}^{-1} = \frac{-34.80 + 10.60}{R} + \frac{56\,200}{RT}; \langle T \rangle = 950 \text{ K} \quad (9)^{15}$$

Virtually the same result is obtained from a “second law” van’t Hoff plot of the data by discarding the lowest temperature equilibrium constant at $T = 858$ K. Least-squares analysis of the remaining body of data gives

$$\ln K_{r,d}/\text{M}^{-1} = \frac{-34.56 + 10.60}{R} + \frac{56\,100}{RT}; \langle T \rangle = 950 \text{ K} \quad (9a)$$

Table I reveals furthermore an average value of k_r of $(1.9 \pm 0.8) \times 10^9 \text{ M}^{-1} \text{s}^{-1}$ at $\langle T \rangle = 880$ K. Thus this method provides a direct measurement of equilibrium (2) with $\Delta S^\circ = -34.56$ eu, $\Delta E^\circ = -56.1$ kcal/mol, and $\Delta H^\circ = -58.0$ kcal/mol. The variable and sometimes large error limits of $K_{r,d}$ displayed in Figure 3 are the result of the algebraic separation of k_r and k_d from two independent experimental sets of k_e^{BA} (large and small apertures) according to (8).¹⁶ The heat capacity data for 1,5-hexadiene¹⁷ and allyl radical¹⁸ are such that ΔS° and ΔH° show no temperature dependence from 300 to 950 K. With $\Delta H^\circ_f(\text{BA}) = 20.2$ kcal/mol (Table II), and $\Delta H^\circ = -58.0 \pm 1.0$ kcal/mol (Figure 3), one obtains $\Delta H^\circ_f(\text{allyl}, g) = 39.1 \pm 1.5$ kcal/mol at $T = 300$ K.¹⁹ The present result indicates an allyl resonance energy (ARE) of 11.7 kcal/mol on the basis of a value of 98.0 kcal/mol for BDE of propane. This is in good agreement with the reported literature values from shock-tube decomposition studies of olefins^{1b-d} and in excellent agreement with a value determined by photoionization mass spectrometry² of 38.4 ± 1.7 kcal/mol for $\Delta H^\circ_f(\text{allyl}, g)$. The agreement with a value of 39.4 ± 1.5 kcal/mol for $\Delta H^\circ_{f,300}$ derived from the measurement of the equilibrium (10) is also noteworthy.²⁰

**Figure 3.** van’t Hoff plot of equilibrium constant $K_{r,d} = k_r/k_d$ for eq 19.**Table II.** Thermochemical Quantities

	$S^\circ_{300}{}^a$	$C_{p,300}{}^a$	$C_{p,625}{}^a$	$C_{p,950}{}^a$	$\Delta H^\circ_{f,300}{}^b$
1,5-hexadiene ^{15,17}	89.40	28.80	50.10	62.44	20.2
allyl radical ¹⁷	62.10	14.60	24.95	30.97	39.1 ^c

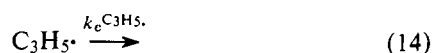
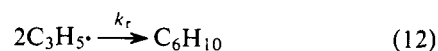
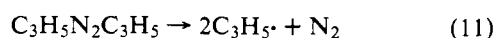
^a cal/K·mol. ^b kcal/mol. ^c Result of present work.

It was pointed out in the Introduction that the earlier study^{1a} of the present system (1)–(5) yielded values for $K_{r,d}$ and k_r somewhat too high, thus providing a value of $\Delta H^\circ_{f,300}(\text{allyl}, g) = 41.2$ kcal/mol and ARE = 9.6 kcal/mol, together with $k_r = 6.2 \times 10^9 \text{ M}^{-1} \text{s}^{-1}$ at 913–1063 K. The reason for this discrepancy was found to lie in a recombination reaction in the mass spectrometry chamber.¹⁰ The present experimental configuration of the apparatus, however, rules out complicating reactions of this kind. The apparent excellent agreement with GVB calculations⁶ should be taken “cum grano salis”, because the “stabilization energy” is referred to the total energy of the hypothetical canonical structure i, which is not an observable species and therefore experimentally not accessible.



The measured value for k_r (9) is discussed together with values obtained at $T = 625$ K in section B.

B. Recombination Kinetics. The recombination kinetics of allyl radical at $T = 625$ K were studied using 3,3'-azo-1-propene (Az) as a source of allyl radicals. The following reaction scheme was assumed:



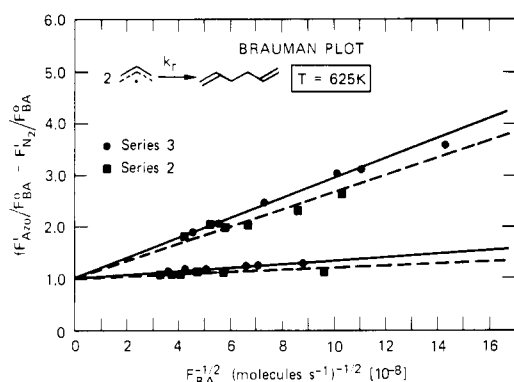


Figure 4. Brauman plot (see text) for the recombination reaction k_r of eq 19 at 625 K (experiments no. 2 and 3, Table III).

The steady-state kinetic expression (the Brauman equation) for the reaction scheme (11)–(14) in a stirred-flow reactor is²¹

$$\frac{F^i_{Az}}{F^0_{BA}} = 1 + \frac{(k_e C_3H_5 + k_w) V^{1/2}}{2k_r^{1/2} F^0_{BA}{}^{1/2}} \quad (15)$$

where F^i_{Az} is the flow (molecules s^{-1}) of 3,3'-azo-1-propene into the reactor, F^0_{BA} is the flow of 1,5-hexadiene out of the reactor (as monitored at m/e 67 or 54), $k_e C_3H_5$ is the escape rate constant (s^{-1}) of allyl radical, and k_w (s^{-1}) is the rate constant for a first-order loss process of the allyl radicals (most likely on the walls). The temperature of 625 K was chosen such that Az was decomposed almost quantitatively, so that the mass spectrometric intensity of m/e 28 (corrected for the contribution of 1,5-hexadiene) reflected the amount of allyl radicals found in the reactor (F^i_{Az}) after assessment of the calibration constant, α_{N_2} (using air), which relates the mass spectral intensity (m/e 28) to the rate of production ($F^i_{N_2} = F^0_{N_2}$) or (steady state) concentration of N_2 .²²

An alternative procedure for determination of F^i_{Az} consisted of "titration" of C_3H_5 with DI (6), while monitoring the mass spectral intensity of m/e 43 (C_3H_5D) under the condition $[DI]_{ss} \rightarrow \infty$, so that the amount of C_3H_5D formed was representative of the amount of allyl radical originally present. However, the concentration of C_3H_5 had to be kept low ($[C_3H_5]_{ss} \approx 3.7 \times 10^{13}$ molecules L^{-1} , corresponding to $F^i_{Az} \approx 5 \times 10^{13}$ molecules s^{-1} at $T = 625$ K), and $[DI]_{ss}$ had to be quite high in view of the smaller rate constant for D transfer (k_3), compared to the recombination rate constant (k_r): $k_r/k_3 \approx 60$ at $T = 625$ K.²⁰ The disappearance of BA in favor of the increase in C_3H_5D could readily be observed at m/e 62, 54 (for BA), and 43 (for C_3H_5D). Both methods of assessing F^i_{Az} gave essentially the same result to within 15%, but the first procedure was used for all reported experiments. A plot of F^i_{Az}/F^0_{BA} vs. $1/F^0_{BA}{}^{1/2}$ gave straight lines according to (15) for two different values of $k_e C_3H_5$ through the common intercept 1.0 (within experimental error; see Figure 4) and indicated that allyl radical was unable to abstract hydrogen in a disproportionation reaction, in line with the results of gas-phase pyrolysis experiments in static high-pressure reaction vessels^{3,7} and the results of section A (eq 7). However, it appears that allyl radical does undergo wall reactions, because the ratio of the slopes for the large and small aperture in Figure 4 is considerably less than the ratio $k_e C_3H_5(B)/k_e C_3H_5(S)$ indicating a nonnegligible term k_w (first-order loss process of allyl radical according to (13), presumably taking place on the walls²³). The results of the pyrolysis of 3,3'-azo-1-propene are displayed in Table III, from which it can be seen that the average value for $k_r = (6.50 \pm 1.0) \times 10^9$ $M^{-1} s^{-1}$ corresponds closely to the one derived at room temperature using kinetic flash spectroscopy⁸ ($k_r = (8.50 \pm 3.0) \times 10^9$ $M^{-1} s^{-1}$).

Table III. Rate Constants for Allyl Radical Recombination at $T = 625$ K

T/K	$k_r/M^{-1} s^{-1}$	k_w/s^{-1}	expt. no.
625	4.31×10^9	3.81	1
625	8.06×10^9	0.58	2
625	7.12×10^9	0.93	3

IV. RRKM Calculations and Discussion

The rate constants for recombination of allyl radicals were calculated using RRKM theory²⁴ for the unimolecular decomposition of 1,5-hexadiene making use of the thermodynamic relation

$$k_r = K_{r,d} k_d \quad (16)$$

Two different transition-state models were used: (1) the vibrational and (2) the rotational model.²⁵

In each case, since the critical energy is known from the equilibrium studies, the other transition-state parameters are adjusted to produce agreement with the recombination rate constant measured at 300 K. Details are discussed below.

In the absence of a complete assignment of the vibrational spectrum of BA, the vibrational frequencies of BA were deduced from those of propylene. The moments of inertia for BA were computed using standard bond lengths and bond angles. The vibrational frequencies were then adjusted so that the computed entropy matched the value from group additivity data.¹⁷ Table IV displays the results of the frequency assignments for BA.

1. The Vibrational Model. In this model for the transition state of the bond-breaking process, the central $-C-C-$ bond was extended 2.5 times²⁶ to 3.85 Å. The torsion around the central $-C-C-$ bond becomes a free rotation of both allyl radical fragments in which resonance stiffening¹⁸ of the former two $C=C$ torsions in BA took place, and the external rotation around the central $-C-C-$ bond was made active to allow these two rotational modes to share in the random distribution of molecular energy. Four $C-C$ rocking modes of the C_3H_5 units in BA had to be replaced by unusually low frequency bending modes (32 cm^{-1}) in order to yield Arrhenius A factors for decomposition of BA which would correspond to the measured rate of recombination⁸ of $(8.50 \pm 3.0) \times 10^9$ $M^{-1} s^{-1}$ at $T = 300$ K through (16); see Table IV. The critical energy for the bond-breaking process (E°_d) was set equal to $-\Delta E^\circ_0$ for equilibrium (2) assuming zero activation energy for recombination (E_r) at 0 K.²⁷ The results of the RRKM calculations are displayed in Figure 5 and are listed in Table V, together with the high-pressure Arrhenius parameters. It is obvious from Figure 5 that the vibrational model successfully fits the experimental data in this case of recombination of two resonance-stabilized radicals. Past experience with the recombination of simple alkyl radicals such as *tert*-butyl, isopropyl, and ethyl has indicated that such a fixed transition-state model was not suited to represent the loose transition state for the bond fission of a simple alkane. The model predicts a transition state with too large a heat capacity at high temperatures owing to the loosening of the four rocking modes in the transition state, thus predicting increasing Arrhenius parameters and increasing values for k_r^∞ with increasing temperatures. The experiments indicate otherwise, however. In the present case of resonance-stabilized radicals, the above increase in heat capacity is essentially balanced by the resonance stiffening of internal rotations, thereby reducing the heat capacity of the transition state. The net result is a small decrease in heat capacity, and a concomitant small decrease in E_d and A_d or a slight negative temperature dependence (see Table V). Although k_r^∞ is seen to increase by a factor of 4 from

Table IV. Molecular Parameters for RRKM Calculations: 1,5-Hexadiene (BA) (Standard State: 1 atm)

	molecule	complex: "vibration"	complex: "rotation"
frequencies	3000 (6)	3010 (2)	3010 (2)
and	2960 (2)	3000 (8)	3000 (8)
degeneracies	2850 (2)	1350 (6)	1350 (6)
	1650 (2)	1300 (6)	1300 (6)
	1470 (2)	1100 (6)	1100 (6)
	1420 (2)	950 (2)	950 (2)
	1400 (2)	400 (4)	350 (2)
	1300 (2)	350 (2)	200 (4)
	1220 (2)	32 (4)	
	1170 (2)		
	920 (3)		
	900 (2)		
	800 (2)		
	350 (2)		
	320 (6)		
	90 (1)		
	70 (1)		
	50 (1)		
$r_{C-C}/\text{\AA}$	1.54	$3.85 (\rho^+ = 2.5)^a$	$3.85 (\rho^+ = 2.5)^a$
$10^{12} I_A I_B I_C / (\text{g cm}^2)^3$	1.78×10^7	8.60×10^7	8.60×10^7
$10^{40} I_r / \text{g cm}^2$		21.20	21.20
$10^{80} I_1 I_2 / (\text{g cm}^2)^2$			$(91.44)^2$
I^+ / I		2.04	2.04
$E^\circ / \text{kcal/mol}$		57.40	57.40
$E_{d,300} / \text{kcal/mol}$		58.15	57.77
$E_{r,300} / \text{kcal/mol}$		0.75	0.37
$S^\circ_{300} / \text{eu}$	88.83	103.19	$103.00; \eta = 99.0\%$
$\log (A_{d,300} / \text{s}^{-1})$		16.37	$16.33; \eta = 99.0\%$
$\log (A_{r,300} / \text{M}^{-1} \text{s}^{-1})$		10.62^b	$10.58; \eta = 99.0\%$

^a $\rho^+ = r^+ / r^0$, where r^+ is the distance of both allyl radical fragments in the activated complex and r^0 is the central C-C bond length in the molecule. ^b $2.303R \log (A_r / \text{M}^{-1} \text{s}^{-1}) / (A_d / \text{s}^{-1}) = -34.60 + 8.32$ with $\delta S^\circ = -34.60$ eu (exptl).

300 to 1000 K, the vibrational model fits the experimental data (k_r) for allyl radical recombination quite satisfactorily in contrast to normal alkyl radicals, where the high-pressure experimental A factors for recombination or bond scission have a pronounced negative temperature dependence.

2. The Rotational Model. This is essentially a Gorin model, which represents the four low-frequency bending vibrations of the two allyl fragments as hindered rotations. The internal modes of the transition state are simply the vibrations and rotations of the independent fragments. This is an alternative picture for the transition state typical of simple bond scission reactions. The hindrance ($\eta/\%$) is accomplished in the calculation by decreasing the effective moment of inertia of each of the two two-dimensional allyl rotors:

$$I_{\text{eff}} = I_1 I_2 \left(\frac{100 - \eta}{100} \right) \quad (17)$$

where I_1 and I_2 are the two one-dimensional component moments of inertia of an allyl fragment excluding the component of the moment of inertia around the axis parallel to the bond being broken. The hindrance effectively decreases the number of available rotational states by confining the rotational motion of each of the fragments. As the centrifugal barrier moves to smaller r^+ values with increasing temperature, η is expected to increase with temperature, thereby²⁶ reducing k_r^∞ . The

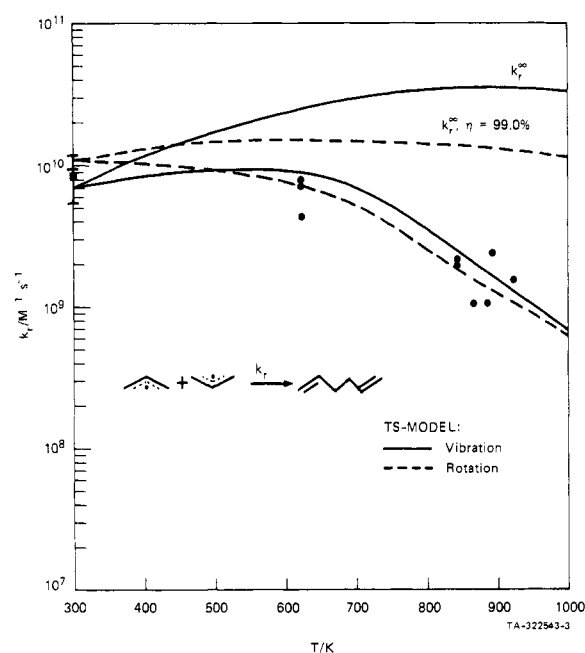


Figure 5. Experimental and calculated rate constants k_r for recombination of allyl radicals as a function of temperature: ■, ref 8; ●, this work; —, vibrational model; - - -, rotational model with hindrance (η) to two-dimensional rotation as indicated in Table V. The pressure corresponds to VLPP gas-collision frequency throughout the whole temperature range ($\omega = 4982(T/\text{M})^{1/2}$).

relation of η to the Arrhenius A factor for decomposition is simply

$$A_H / A = \frac{100 - \eta}{100} \quad (18)$$

where A_H is the A factor derived from a transition state model with $\eta \neq 0$. In the case of the rotational model, the same molecular parameters were chosen as for (1), $E_d^\circ = -\Delta E^\circ_0 = -\Delta E^\circ_T + T\langle\Delta C_v\rangle$, except that the four low-frequency bending modes at 32 cm^{-1} were replaced by two two-dimensional rotations of the allyl fragments ($I_{\text{eff}} = 8.36 \times 10^{83} [(100 - \eta)/100] (\text{g cm}^2)^2$) along with two other minor changes in the lower frequencies. It was found that a good fit to the experimental data could be obtained by choosing a constant value for η of 99%. Table V shows the results of the calculation and Figure 5 displays the corresponding plot together with the experimental rate constants k_r and k_r^∞ . Not too much importance should be attached to the absolute value of η , because this number is dependent on the details of the transition-state model with respect to its structure and the vibrational frequencies.²⁸ Table V describes, therefore, only a "reasonable" choice of molecular parameters for transition states (1) to (2). Furthermore, the exact relationship between η and the geometrical parameters of the fragments (rotational "freedom" or tightness) in the transition state is virtually unknown. It should be noted that in this case no dependence of η on temperature is found experimentally, in contrast to three recent examples.²⁵ For methyl radical recombination, η increases from 63 to 82% over the temperature range 300–1400 K. In the case of the recombination of HO_2^\cdot with NO_2^\cdot , η varies from 92 to 98% over the temperature range 217–300 K, and in the recombination of *tert*-butyl radical with methyl radical, η changes from 75% at 300 K to 98.7% at 200 K.

An intuitive choice for the interfragment distance in the critical configuration of a normal alkane undergoing bond fission to two alkyl radicals would be the top of the centrifugal barrier.^{17,26} Recent calculations on ethane dissociation suggest, however, that the application of the criterion of minimum

Table V. Results of RRKM Calculations for the Bond-Breaking Process 1,5-Hexadiene \rightarrow 2 Allyl Radical at Selected Temperatures^a

<i>T</i> /°K	ΔE° kcal/mol	$K_{r,d}/M^{-1}$	vibrational model (1)						rotational model (2)					
			$\log(A_d/s^{-1})$	E_d	E_r	k_d/s^{-1}	k_r/M^{-1} s^{-1}	k/k^∞	$\log(A_d/s^{-1})$	E_d	E_r	k_d/s^{-1}	k_r/M^{-1} s^{-1}	k/k^∞
300	57.40	6.93×10^{35}	16.37	58.15	0.75	0.102×10^{-25}	7.00×10^9	0.988	$\eta = 99.0\%$ 16.38	57.77	0.37	0.125×10^{-25}	8.66×10^9	0.991
625	56.75	2.12×10^{14}	16.30	58.00	1.25	0.424×10^{-4}	9.00×10^9	0.370	$\eta = 99.0\%$ 15.65	56.58	-0.17	0.585×10^{-4}	6.25×10^9	0.503
800	56.40	1.06×10^{10}	16.26	57.90	1.50	0.313	3.32×10^9	0.101	$\eta = 99.0\%$ 15.37	55.85	-0.35	0.202	2.14×10^9	0.192
900	56.20	2.12×10^3	16.25	57.84	1.64	7.35	1.56×10^9	0.0449	$\eta = 99.0\%$ 15.26	55.41	-0.79	4.87	1.03×10^9	0.0987
950	56.10	4.10×10^7	16.24	57.80	1.70	25.23	1.03×10^9	0.0304	$\eta = 99.0\%$ 15.20	55.48	-0.92	16.84	6.90×10^8	0.0718

^a $\Delta S^\circ_r = +34.60$ eu from $T = 300$ to 1000 K; collision frequency $\omega = 4982(T/M)^{1/2}$.

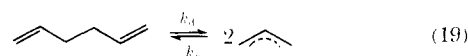
density of states²⁹ is more appropriate in locating the critical configuration with respect to the reaction coordinate. If no other structural changes in the molecule occur during the bond split, the location of the minimum density of states will coincide with the location of the top of the centrifugal barrier. As the C-C bond is breaking, however, lowering of the rocking mode frequencies is expected to occur. Loosening of these vibrations in the molecule will shift the location of the minimum density of states toward smaller values of the reaction coordinate, and alternatively stiffening of internal modes will shift the minimum density of states to larger values of the reaction coordinate as compared to the location of the centrifugal barrier.²⁹ As the temperature goes up, the minimum density of states, as well as the top of the rotational barrier, moves to smaller values of the interfragment distance. The -C-C- bond scission in 1,5-hexadiene to two resonance-stabilized allyl radicals is a case in which the anticipated loosening of internal modes upon bond breaking is accompanied by a concomitant "resonance stiffening", mainly of the free internal rotations, resulting in a near cancellation of the temperature dependence of the location of the minimum density of states. The near balance of two opposing effects, namely, loosening and stiffening of internal modes in the critical configuration of 1,5-hexadiene upon bond breaking, and its apparent lack of temperature sensitivity resembles the temperature-independent vibrational model. This balance is thus thought to be the main reason for η being constant (within experimental error) over the temperature range 300–1000 K, and thus for the transition state being fixed with increasing temperature. The explanation put forward above is of a qualitative nature and warrants further detailed calculations on the 1,5-hexadiene system. The foregoing discussion makes it clear why a vibrational model is equally successful in describing the bond scission of 1,5-hexadiene. In this case, both the vibrational and rotational models are characterized by the same (negative) temperature dependence of their respective Arrhenius parameters, though to a different degree (see Table V), whereas in contrast to experimental results in the case of a C-C bond split in an alkane, the vibrational model predicts a strong positive temperature dependence of its Arrhenius parameters.

A glance at the high-pressure Arrhenius parameters E_d and $\log A_d$ for model (2), Table V, reveals that the rotational model has only $4R/2$ heat capacity associated with its hindered rotations, such that E_d and $\log A_d$ decrease by 2.36 kcal/mol and 1.07 logarithmic units, respectively, over the temperature range 300–900 K. With this method of calculation (i.e., choosing an A factor at $T = 300$ K to match the low-temperature recombination rate constant and subsequent extrapolation of the rate constant with the rotational transition state model), one is led to conclude that the system has a negative activation energy for recombination ($E_r = -0.80$ kcal/mol) at $T = 900$ K.²⁷ This is an artifact of the model, however, and is clearly the consequence of lacking heat capacity of the four

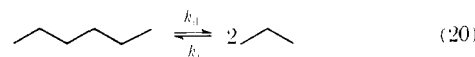
hindered rotations. No attempt has been made, however, to associate an increased amount of heat capacity with these hindered internal rotations, knowing that the upper limit with respect to the heat capacity of the activated complex is represented in the vibrational model (1). With the present fall-off data for recombination of allyl radical, no unambiguous choice between transition state models (1) or (2) can be made. We are inclined to favor at this point the simple vibrational transition state model (1).

Tsang^{1c} estimated the Arrhenius parameters for the bond scission of BA at 1100 K ($\log A_d = 14.20$, $E_d = 59.3$ kcal/mol), through the application of the usual geometric mean rule for the cross combination to combination ratio r ($r = k_r(AB)/(k_r(AA)k_r(BB))^{1/2}$). Using the estimated value of 14.20 for $\log A_d$, together with the overall entropy change (ΔS°) of -34.6 eu and the change in internal energy (ΔE°) of 56.0 kcal/mol at $T = 1000$ K, yields $\log k_r = 8.26$ (Table VI, reaction 4), which is 1.5–2 orders of magnitude too low in light of our results.³⁰ If the rate constant for allyl + CH_3 recombination is set equal to $10^{10.30}$ (see Table VI, reaction 2), one would predict a value of 0.79 or 1.41 for r , instead of 2.45 (as used by Tsang), on the basis of our measured value for k_r^∞ , which is subject to the choice of the appropriate transition-state model. We favor a value of $r = 0.79$ as a result of our preferred choice of the vibrational model (vide supra). A recent pyrolysis study of 1,1'-azoisobutane³² provided an experimental value of $r = 0.25$ for the methyl plus isobutyl radical pairs. The results of the flash photolysis study of 2-methylbutene-1, where $r = 0.09$ was found, seem too low and may indicate an experimental problem. Adjustment of r to higher values in this case would decrease k_r for reaction (3), Table VI, which seems somewhat high in view of the results for allyl radical recombination of Van den Bergh and Callear⁸ at 300 K, and/or concomitantly would increase k_r for reaction 2, Table VI, which seems unusually low for the cross-combination rate constant. These few examples show that $r = 2.0$ may not always be valid without prior experimental assessment of the involved rate constants.

Finally, we would like to point out that $\log A_d/s^{-1}$ values for reactions 19 and 20 are 16.00 and 15.70 logarithmic units








$T = 300$ K; $\log k_r = 9.93$ (ref 8); $E_r = +0.5$ kcal/mol (cf. Table V)



$T = 300$ K; $\log k_r = 10.00$ (assumed); $E_r = +0.5$ kcal/mol (assumed)

at 300 K and are thus roughly equal by virtue of their almost equal overall entropy of reaction ($\Delta S^\circ = 34.60$ for (19), ΔS°

Table VI. Experimental and Calculated Recombination Rate Constants for Radical Recombination Reactions Involving Stabilized Radicals

no. recombination reaction	$T/^{\circ}\text{K}$	$\log(k_r(\text{exptl})/\text{M}^{-1}\text{s}^{-1})$	$\log(k_r(\text{GM})^a/\text{M}^{-1}\text{s}^{-1})$	ref	remarks
1 $\text{CH}_3\cdot + \text{CH}_3\cdot \rightarrow \text{C}_2\text{H}_6$	1000 300	10.30 10.38		31 31	
2  + $\text{CH}_3\cdot \rightarrow \text{C}_5\text{H}_{10}$	1020 300	10.30 9.35		1d 9	flash photolysis study
3  +  $\rightarrow \text{C}_8\text{H}_{14}$	300 1000 300	10.41		9	flash photolysis shock-tube data ^{1d} reaction 2 data of ref 9 for reaction 2
4  +  $\rightarrow \text{C}_6\text{H}_{10}$	1000 1000	10.50 ^b 10.00 ^c		this work	
	1000		8.26	1c	using A_d of ref 1c and ΔS° (ref 17 and 18) for overall reaction to compute k_r^d

^a Value for $k_r(\text{AB})/k_r^{1/2}(\text{AA})k_r^{1/2}(\text{BB})$ (geometric mean rule) is assumed to be 2.00.^{1c} ^b Vibrational transition state. See Figure 5. ^c Rotational transition state. See Figure 5. ^d $2.303R \log [(A_r/\text{M}^{-1}\text{s}^{-1})/(A_d/\text{s}^{-1})] = -34.60 + 10.74$. At $T = 1000\text{ K}$, $k_r(\text{exptl}) = A_r e^{-3.3/2}$ with $E_r = 3.3\text{ kcal/mol}$, and $\log A_r = 8.98$ to yield $\log k_r = 8.26\text{ M}^{-1}\text{s}^{-1}$.

= 32.70 eu for (20)) and rate of recombination ($\text{M}^{-1}\text{s}^{-1}$).

We conclude, therefore, that the present "high" value for the recombination rate, which is quite similar in magnitude to common alkyl radical recombination rate constants (ethyl radical recombination, $k_r = (7.80 \pm 1.80) \times 10^9\text{ M}^{-1}\text{s}^{-1}$ at room temperature, ref 33) is indicative of the fact that the recombination reaction shows no apparent activation energy and that the delocalization of the unpaired electron has no effect on the recombination rate of allyl radical.

V. Summary

This study yields $\Delta H^{\circ}_{f,300}(\text{allyl}) = 39.1 \pm 1.5\text{ kcal mol}^{-1}$, and thus an allyl resonance energy $\text{ARE} = 11.7 \pm 2.0\text{ kcal mol}^{-1}$. At the same time, these results yield a value for k_r^{∞} which is about the same as for alkyl radicals, indicating no effect of the electron delocalization on reactivity.

Acknowledgment. We would like to thank Dr. G. Manser, who provided us with a sample of 3,3'-azo-1-propene. Also, Dr. Keith D. King wishes to thank the Australian-American Educational Foundation for the award of a Fulbright Travel Grant. This work was supported, in part, by Contract F44620-75-C-0067 with the Air Force Office of Scientific Research.

Appendix

The steady-state kinetic expressions for the reaction system (1)–(5) in a stirred-flow reactor shall now be derived.

Under steady-state conditions, the following expressions for the concentration of the involved species result:

$$d(\text{DAO})/dt = R^i_{\text{DAO}} - k_1(\text{DAO}) - k_e^{\text{DAO}}(\text{DAO}) \equiv 0 \quad (\text{A1})$$

$$d(\text{CO}_2)/dt = 2k_1(\text{DAO}) - k_e^{\text{CO}_2}(\text{CO}_2) \equiv 0 \quad (\text{A2})$$

$$d(\text{C}_3\text{H}_5\cdot)/dt = 2k_1(\text{DAO}) + 2k_d(\text{BA}) - 2k_r(\text{C}_3\text{H}_5\cdot)^2 - k_e^{\text{C}_3\text{H}_5\cdot}(\text{C}_3\text{H}_5\cdot) \equiv 0 \quad (\text{A3})$$

$$d(\text{BA})/dt = k_r(\text{C}_3\text{H}_5\cdot)^2 - k_d(\text{BA}) - k_e^{\text{BA}}(\text{BA}) \equiv 0 \quad (\text{A4})$$

where R^i_P is the flow of the species P into the reactor (in units of molecules $\text{s}^{-1}\text{ L}^{-1}$), k^P_e is the escape rate constant of P out of the reactor, and DAO stands for diallyl oxalate and BA for 1,5-hexadiene.

Rearrangement of (A4) yields

$$(\text{BA})/(\text{C}_3\text{H}_5\cdot)^2 = k_r/(k_d + k_e^{\text{BA}}) \quad (\text{A5})$$

Keeping in mind that $R^0_P = k^P_e(P)$, where R^0_P is the flow of species P out of the reactor, the combination of (A3) and (A4) results in (A6) using the substitution $2k_1(\text{DAO}) = R^0_{\text{CO}_2}$ from (A2):

$$\frac{(\text{BA})}{(\text{C}_3\text{H}_5\cdot)^2} = \frac{(k_e^{\text{C}_3\text{H}_5\cdot})^2(\text{BA})}{(k_e^{\text{CO}_2}(\text{CO}_2) - 2k_e^{\text{BA}}(\text{BA}))^2} \quad (\text{A6})$$

Comparison of (A6) and (A5) results in the desired expression

$$\frac{k_r}{k_d + k_e^{\text{BA}}} = k_e^{\text{BA}} \frac{2R^0_{\text{BA}}}{(R^0_{\text{CO}_2} - 2R^0_{\text{BA}})^2} \quad (\text{A7})$$

which enables one to establish $k_r/(k_d + k_e^{\text{BA}})$ with the experimental values of R^0_{BA} and $R^0_{\text{CO}_2}$. With two independent values of k_e^{BA} (e.g., corresponding to a large and a small aperture in the VLPP reactor), the algebraic separation of k_r and k_d is possible.

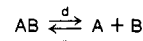
References and Notes

- (1) (a) D. M. Golden, N. A. Gac, and S. W. Benson, *J. Am. Chem. Soc.*, **91**, 2136 (1969), and references cited therein; (b) W. Tsang, *J. Chem. Phys.*, **46**, 2817 (1967); (c) *Int. J. Chem. Kinet.*, **1**, 245 (1969); (d) *ibid.*, **5**, 929 (1973); (e) W. M. Marley and P. M. Jeffers, *J. Phys. Chem.*, **79**, 2085 (1975).
- (2) S. E. Buttrill, A. D. Williamson, and P. LeBreton, *J. Chem. Phys.*, **62**, 1586 (1975).
- (3) A. B. Trenwith and S. P. Wrigley, *J. Chem. Soc., Faraday Trans. 1*, **73**, 817 (1977), and references cited therein.
- (4) Defining the bond dissociation energy for any bond A–B, $\text{DH}^{\circ}_{f, \tau}(\text{A–B}) = \Delta H^{\circ}_{f, \tau}(\text{A}) + \Delta H^{\circ}_{f, \tau}(\text{B}) - \Delta H^{\circ}_{f, \tau}(\text{A–B})$, we may define the stabilization energy in the allyl radical (ARE) as $\text{DH}^{\circ}_{300}(n\text{-C}_3\text{H}_7\text{–H}) - \text{DH}^{\circ}_{300}(\text{allyl–H}) \equiv \text{ARE}$.
- (5) J. M. McKelvey and G. Berthier, *Chem. Phys. Lett.*, **41**, 426 (1976), and references cited therein.
- (6) G. Levin and W. A. Goodard III, *J. Am. Chem. Soc.*, **97**, 1649 (1975); *Theor. Chim. Acta*, **37**, 253 (1975).
- (7) J. A. Kerr in "Free Radicals", Vol. 1, J. K. Kochi, Ed., Wiley, New York, 1973, Chapter 1.
- (8) H. E. Van den Bergh and A. B. Callear, *Trans. Faraday Soc.*, **66**, 2681 (1970).
- (9) F. Bayrakceken, J. H. Brophy, R. D. Fink, and J. E. Nicholas, *Trans. Faraday Soc.*, **68**, 228 (1972).
- (10) In ref 1a, a somewhat older version of the VLPP apparatus without molecular beam-sampling phase-sensitive detection was used. The different results obtained by Golden et al. could be accounted for by wall-catalyzed recombination of allyl radicals on the walls of the mass spectrometry chamber. We get essentially the results of ref 1a without phase-sensitive detection, i.e., a higher value for $K_{r,d}$ at these temperatures.
- (11) D. M. Golden, G. N. Spokes, and S. W. Benson, *Angew. Chem.*, **85**, 602 (1973).
- (12) B. H. Al-Sader and R. J. Crawford, *Can. J. Chem.*, **48**, 2745 (1970); R. J. Crawford and K. Takagi, *J. Am. Chem. Soc.*, **94**, 7406 (1972).
- (13) D. G. L. James and S. M. Kambanis, *Trans. Faraday Soc.*, **65**, 1350 (1969).

- (14) At every temperature the calibration factor α_j in $\mu = \alpha_j k_e / [j]_{ss}$, where j is *m/e* 67, 54 (1,5-hexadiene), and 44 (CO_2), was determined by at least two different flow rates $k_e/[j]_{ss} = F_j$. α_j relates mass spectrometric intensities (μ) to steady-state concentrations of a molecule ($[j]_{ss}$).
- (15) $\ln(K_{r,d}/\text{M}^{-1}) = [\Delta S^\ddagger - \Delta nR(1 + \ln(R'/T))]/R - \Delta E^\ddagger/RT$, where the superscript refers to a standard state of 1 atm and R' distinguishes the gas constant in units of L atm/mol K from units of cal/mol K.
- (16) Defining $z_s = y_s k_e^{\text{BA}}(\text{S})$, $z_B = y_B k_e^{\text{BA}}(\text{B})$, and $K_{r,d} = k_r/k_d$, the propagation of errors yields for the relative error of $K_{r,d}$ the following expression:
- $$\frac{\Delta K_{r,d}}{K_{r,d}} = \left(2 \left(\frac{\Delta z_B + \Delta z_s}{z_B k_e^{\text{BA}}(\text{B}) - z_s k_e^{\text{BA}}(\text{S})} \right)^2 + 2 \left(\frac{\Delta z_B + \Delta z_s}{z_B - z_s} \right)^2 + \left(\frac{\Delta z_B}{z_B} \right)^2 \right)^{1/2}$$
- (17) S. W. Benson, "Thermochemical Kinetics", 2nd ed., Wiley, New York, 1976.
- (18) H. E. O'Neal and S. W. Benson, *Int. J. Chem. Kinet.*, **1**, 217 (1969).
- (19) The uncertainty in ΔH° from the equilibrium measurements (2) is estimated to be ± 1 kcal/mol. Together with the uncertainty in $\Delta H^\circ_f(\text{BA})$ of ± 0.5 kcal/mol, the combined uncertainty for $\Delta H^\circ_f(\text{allyl}, \text{g})$ amounts to ± 1.5 kcal/mol.
- (20) M. Rossi and D. M. Golden, *J. Am. Chem. Soc.*, following paper in this issue.
- (21) K. Y. Choo, P. C. Beadle, L. W. Piszkiwicz, and D. M. Golden, *Int. J. Chem. Kinet.*, **8**, 45 (1976).
- (22) $I_{\text{N}_2}^{\text{N}_2} = \alpha_{\text{N}_2} k_e^{\text{N}_2} [\text{N}_2]_{ss} = \alpha_{\text{N}_2} F_{\text{N}_2}^{\text{N}_2} = \alpha_{\text{N}_2} F_{\text{N}_2}^{\text{N}_2}$. For explanation of symbols, see ref 14.
- (23) Experiment no. 1 in Table III was performed at an earlier stage of the recombination series than no. 2 and 3, indicating variable wall conditions of the reaction vessel within the series of experiments.
- (24) P. J. Robinson and K. A. Holbrook, "Unimolecular Reactions", Wiley-Interscience, New York, 1972.
- (25) (a) G. P. Smith, M. Lev-On, and D. M. Golden, submitted for publication; (b) A. C. Baldwin and D. M. Golden, *J. Phys. Chem.*, **82**, 644 (1978); (c) A. C. Baldwin, K. E. Lewis, and D. M. Golden, *Int. J. Chem. Kinet.*, submitted.
- (26) The separation distance along the bond axis was chosen in such a way that it corresponded to the top of the centrifugal barrier in a model for a Lennard-Jones potential of the C-C bond connecting both C_3H_5 units: $\rho^+ =$

$r^+/r_0 = (6D_0/RT)^{1/6}$. This rotational maximum of the effective potential, including rotation, is not very sensitive to either T or the precise value of D_0 , and for most common values of both occurs in the range $\rho^+ = 2.5$ –3.0.

- (27) For any reaction



$$\begin{aligned} \Delta E^\circ_0 &= E^\circ_d - E^\circ_r \equiv E^\circ_{\text{d}} = \Delta E^\ddagger_{\text{o,d}} \equiv \text{critical energy} \\ E^\ddagger_{\text{d}} &\equiv \Delta E^\ddagger_{\text{T,d}} + RT = \Delta E^\ddagger_{\text{o,d}} + \langle \Delta C^\ddagger_{\text{v,d}} \rangle T_0 T + RT \\ E^\ddagger_{\text{d}} &= \Delta E^\circ_0 + \langle \Delta C^\ddagger_{\text{v,d}} \rangle T_0 T + RT \end{aligned}$$

since

$$\begin{aligned} \Delta E^\circ_0 &= \Delta E^\circ_T - \langle \Delta C_v \rangle T_0 T \\ E^\ddagger_{\text{d}} &= \Delta E^\circ_T - \langle \Delta C_v \rangle T_0 T + \langle \Delta C^\ddagger_{\text{v,d}} \rangle T_0 T + RT \\ E^\ddagger_{\text{d}} &= \Delta H^\circ_T + \langle \Delta C^\ddagger_{\text{v,r}} \rangle T_0 T \end{aligned}$$

- (28) Given η and $I_{\text{A}}/I_{\text{B}}/I_{\text{C}}$ for a rotational model transition state, changing $I_{\text{A}}/I_{\text{B}}/I_{\text{C}}$ to $I_{\text{A}}'/I_{\text{B}}'/I_{\text{C}}'$ results in a different hindrance parameter (η') to yield the same Arrhenius A factor through the following relation:

$$\eta' = 100 - (100 - \eta) \left(\frac{I_{\text{A}}'/I_{\text{B}}'/I_{\text{C}}'}{I_{\text{A}}/I_{\text{B}}/I_{\text{C}}} \right)$$

If $I_{\text{A}}'/I_{\text{B}}'/I_{\text{C}}' > I_{\text{A}}/I_{\text{B}}/I_{\text{C}}$, it then follows that $\eta' < \eta$.

- (29) W. L. Hase, *J. Chem. Phys.*, **64**, 2442 (1975); W. L. Hase in "Dynamics of Molecular Collisions", W. H. Miller, Ed., Plenum Press, New York, 1976.
- (30) $k_r(\text{exp}) = A_r e^{-3.3/2}$ at $T = 1000$ K with $E_r = 3.3$ kcal/mol from $E_0 = 59.3$ kcal/mol, and $\Delta E = 56.0$ kcal/mol.
- (31) See references in ref 22a; S. W. Benson and H. E. O'Neal, *Natl. Stand. Ref. Data Ser., Natl. Bur. Stand.*, **No. 21** (1970).
- (32) G. McKay and I. M. C. Turner, *Int. J. Chem. Kinet.*, **10**, 89 (1978).
- (33) D. A. Parkes and C. R. Quinn, *J. Chem. Soc., Faraday Trans. 1*, **72**, 1952 (1976).

Absolute Rate Constants for Metathesis Reactions of Allyl and Benzyl Radicals with HI (DI). Heat of Formation of Allyl and Benzyl Radicals

M. Rossi[†] and D. M. Golden*

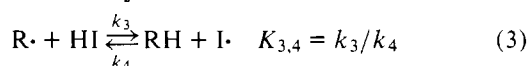
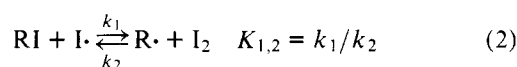
Contribution from the Thermochemistry and Chemical Kinetics Group, SRI International, Menlo Park, California 94025. Received May 4, 1978

Abstract: The metathesis reaction $\text{C}_3\text{H}_5\cdot + \text{HI} (\text{DI}) \rightarrow \text{C}_3\text{H}_6 (\text{C}_3\text{H}_5\text{D}) + \text{I}\cdot (k_3)$ has been studied in the gas phase using the VLPP technique. The result with DI, using diallyl oxalate as a radical source, is $\log(k_3/\text{M}^{-1}\text{s}^{-1}) = (10.11 \pm 0.30) - (5.7 \pm 1.5)/\theta$ at $T = 1000$ K. The result using 3,3'-azopropene as a radical source is $\log(k_3/\text{M}^{-1}\text{s}^{-1}) = 8.93 \pm 0.18$ at $T = 1000$ K, where $\theta = 2.303RT$ in kcal mol⁻¹. For the metathesis reaction $\text{C}_6\text{H}_5\text{CH}_2\cdot + \text{DI} \rightarrow \text{C}_6\text{H}_5\text{CH}_2\text{D} + \text{I}\cdot (k_3)$, $\log(k_3/\text{M}^{-1}\text{s}^{-1}) = (10.46 \pm 0.30) - (6.3 \pm 1.5)/\theta$ at $T = 1000$ K. These rate expressions were extrapolated to lower temperatures using a transition-state model in order to compute the equilibrium constants for the above metathesis reactions using the rate constants for the reverse metathesis from iodination studies. The equilibrium constants yield $\Delta H^\circ_f(\text{allyl}) = 39.4 \pm 1.5$ kcal/mol and $\Delta H^\circ_f(\text{benzyl}) = 47.80 \pm 1.5$ kcal/mol at $T = 300$ K. These values correspond to stabilization energies of 11.4 ± 1.5 and 10.1 ± 2.0 kcal/mol, respectively (i.e., $\text{DH}(\text{allyl-H}) = 86.6 \pm 1.5$ kcal/mol and $\text{DH}(\text{C}_6\text{H}_5\text{CH}_2\text{-H}) = 87.9 \pm 1.5$ kcal/mol).

I. Introduction

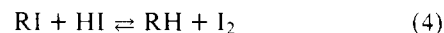
A large number of values for free-radical heats of formation ($\Delta H^\circ_f(\text{R}\cdot)$) have been obtained by the spectrophotometric iodination technique which is well documented in the literature.¹

The pertinent reactions are



[†] Postdoctoral Research Associate.

with the following overall equilibrium:



In general, the temperature-dependent values of k_1 and k_2/k_3 (starting with $\text{RI} + \text{HI}$) or k_4 and $K_{3,4}$ (starting with $\text{RH} + \text{I}_2$) can be obtained. The usual method of extracting $\Delta H^\circ_f(\text{R}\cdot)$ from these studies is to assume that $E_2 = 0.0 \pm 1.0$ kcal/mol and/or $E_3 = 1.0 \pm 1.0$ kcal/mol. (The measured values of $E_2 - E_3$ are not inconsistent with these assumptions). Thus, a measurement of E_4 will yield a value for $\Delta H^\circ_{3,4}$ and $\Delta H^\circ_f(\text{R}\cdot)$ will follow since the appropriate values for HI , $\text{I}\cdot$ and RH are known.²

Very low-pressure pyrolysis (VLPP) allows the measurement of fast bimolecular reactions such as (5) in the gas phase.